Electronic Supplementary Information

Optical Kerr Effect Spectroscopy of CS_2 in Monocationic and Dicationic Ionic Liquids: Insights into the Intermolecular Interactions in Ionic Liquids

Eshan Gurung,[1] Dujuan Meng,[1] Lianjie Xue,[1] George Tamas,[1] Ruth M. Lynden Bell,[2] Edward L. Quitevis[1]*

[1]Department of Chemistry & Biochemistry, Texas Tech University. Lubbock, TX 79409

[2]Department of Chemistry, University of Cambridge, Lensfield Road, Cambridge, CB2 1EW, UK

*Corresponding author: edward.quitevis@ttu.edu

I. Synthesis of Ionic Liquids

All reagents and solvents were acquired from commercial sources (Acros Organics, 3M and Sigma-Aldrich) and were used as received, without further purification. All reactions were run under nitrogen atmosphere, using oven-dried glassware. NMR spectra were recorded on a JEOL 400 spectrometer and collected as solutions of deuterochloroform (bromide ionic liquids) or deuteroacetone (bistriflate ionic liquids).

A. Synthesis of 1-alkyl-3-methylimidazolium bis[(trifluoromethane)sulfonyl]amide ionic liquids [$C_nC_1$im][NTf_2].

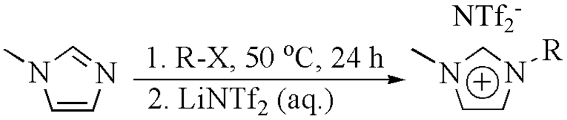

Scheme 1. Generic synthesis of [$C_nC_1$im][NTf_2] for n = 3-5.

All ionic liquids were synthesized using modified procedures published elsewhere and following the generic scheme presented above.[1,2] The quaternization step was performed at 50 °C, adding a slight excess of the corresponding alkyl bromide (*i.e.,* 1.05 eq.) to ensure complete consumption of 1-methylimidazole. The unreacted halide was removed by repeated washing of the ionic liquid with a 1: 3 (v/v) mixture of dichloromethane and hexanes. The decolorization of the ionic liquid was accomplished at the bromide stage according to an in-house developed protocol (*vide infra*). The metathesis was performed in presence of aqueous lithium bis[(trifluoromethane)sulfonyl]amide ($LiNTf_2$).[3] The lithium bromide formed was removed by repeated washing with triple deionized water until passing the silver nitrate test. The excess water was removed *via* benzene azeotrope, using a Dean-Stark trap. Further drying was carried out under high vacuum at 40 °C and having the water content assessed by Karl-Fischer titration. All final products were colorless liquids at room temperature.

B. Synthesis of 1,n-bis(3-methylimidazolium-1-yl)alkane bis[(trifluoromethane)sulfonyl]amide ionic liquids $[(C_1im)_2C_n][NTf_2]_2$

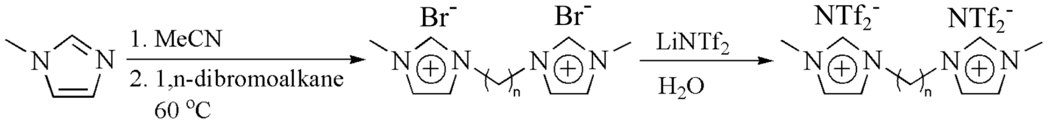

Scheme 2. Generic synthesis of $[(C_1im)_2C_n][NTf_2]_2$ for n = 6, 8, and 10.

A two-neck round bottom flask, under nitrogen, equipped with a magnetic stirrer and a condenser, was charged with 50 mL of acetonitrile and 2.1 eq. of 1-methylimidazole. To this closed system, the corresponding dibromoalkane (1 eq.), dissolved in 10 mL of acetonitrile, was delivered dropwise at a rate of 0.34 mL/min with an automatic syringe. The reaction was left under constant stirring at 60 °C until complete consumption of the dibromoalkane. After the completion of the addition, a white slurry was formed. The product, $[(C_1im)_2C_n][Br]_2$, was vacuum filtered, rinsed with diethyl ether and then the solvent evaporated *in vacuo.* The solid formed was further dried on a Schlenk line. The last stage of synthesis was accomplished *via* metathesis reaction.[3] An aqueous solution of $LiNTf_2$ (1.98 eq.) was added to the dibromide IL and left to stir overnight. The two-phase system was then repeatedly washed with triple-deionized water until no bromide ions could be detected by the silver nitrate test. The final product, $[(C_1im)_2C_n][NTf_2]_2$, was dried with a benzene azeotrope. The residual benzene was removed under vacuum. For decolorization, 3 g of activated charcoal and 60 mL of acetonitrile were added to the viscous, slightly yellow IL, and left under stirring for 96 h. The black slurry was then filtered through a gravitational column packed with 10 cm of aluminum oxide (activated, basic, 50-200 micron) and 3 cm of celite 545. The removal of the solvent under reduced pressure afforded the dicationic ionic liquid as a colorless, viscous liquid at room temperature. Yields: 74 - 86%.

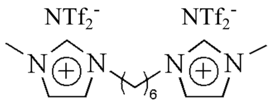

$[(C_1im)_2C_6][NTf_2]_2$

1,6-Bis(3-methylimidazolium-1-yl)hexane bis[(trifluoromethane)sulfonyl]amide

^{1}H NMR (400 MHz, Acetone-*d*$_6$) δ: 8.99 (s, 2H), 7.74 (t, *J* = 1.83 Hz, 2H), 7.70 (t, *J* = 1.83 Hz, 2H), 4.35 (t, *J* = 7.33 Hz, 4H), 4.04 (s, 6H), 2.02-1.92 (m, 4H), 1.48-1.44 (m, 4H)

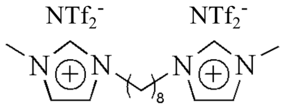

$[(C_1im)_2C_8][NTf_2]_2$

1,8-Bis(3-methylimidazolium-1-yl)octane bis[(trifluoromethane)sulfonyl]amide

^{1}H NMR (400 MHz, Acetone-*d*$_6$) δ: 8.95 (s, 2H), 7.72 (t, *J* = 1.83 Hz, 2H), 7.67 (t, *J* = 1.83 Hz, 2H), 4.32 (t, *J* = 7.12 Hz, 4H), 4.03 (s, 6H), 1.97-1.89 (m, 4H), 1.35 (s, br, 8H)

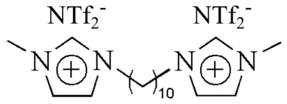

$[(C_1im)_2C_{10}][NTf_2]_2$

1,10-Bis(3-methylimidazolium-1-yl)decane bis[(trifluoromethane)sulfonyl]amide

^{1}H NMR (400 MHz, Acetone-*d*$_6$) δ: 8.96 (s, 2H), 7.72 (t, *J* = 1.83 Hz, 2H), 7.67 (t, *J* = 1.83 Hz, 2H), 4.33 (t, *J* = 7.33 Hz, 4H), 4.04 (s, 6H), 1.97-1.89 (m, 4H), 1.36-1.28 (m, 12H)

II. OHD-RIKES Time-Domain Data

Shown in Figure S1 are semi-logarithmic plots of representative OHD-RIKES signals in the 0-4 ps time range for the neat liquids, CS_2, MIL(3), and MIL(6), and the mixtures, CS_2/MIL(3) and CS_2/DIL(6). The signals are height normalized at the coherent spike at $t = 0$ in order to compare the decay pattern of the neat liquids to that of the mixtures. The instantaneous electronic response (the coherent spike) is the sharp peak at zero-time delay and the non-instantaneous part is the nuclear response. The OHD-RIKES signal for neat ILs at early times is dominated by the instantaneous electronic component (i.e., coherent spike), in comparison to the non-instantaneous nuclear component. In contrast, for neat CS_2, the electronic and nuclear components contribute equally to the Kerr response at early times. Because a 50-fs step size is used in the time window between -1 and 4 ps, the rapid oscillations arising the coherent excitation of intramolecular vibration modes of the cation and anion appear in the Kerr transients. In both CS_2/IL mixtures, the amplitude of the nuclear response relative to that of electronic response increases with the increase in mole fraction of CS_2.

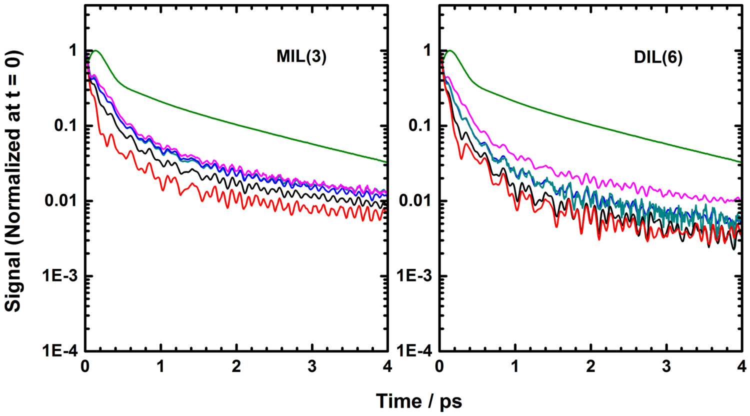

Figure S1. Representative semi-logarithmic plots of the OHD-RIKES signals in the 0-4 ps time range for CS_2/MIL(3) mixtures, top to bottom mol %: 100, 25, 20, 15, 10 , 0. and CS_2/DIL(6), top to bottom mol %: 100, 40, 33.3, 26, 18.2, 0. Signals have been normalized at the coherent spike at $t = 0$.

Shown in Figure S2 are representative OHD-RIKES signals in the 0-10 ps time range for neat liquids CS_2, MIL(3), and DIL(6), and for the mixtures 10 mol.% CS_2/MIL(3) and 18.2 mol.% CS_2/DIL(6) mixtures. In the case of neat CS_2, the long-time part (t >1 ps) of the nuclear response decays exponentially to baseline. In contrast, for the neat ILs and CS_2/IL mixtures, the long-time part of the nuclear response decays non-exponentially and is not fully relaxed. OHD-OKE measurements[4-6] over a much longer time range than in the current study indicate that the slow non-exponential relaxation of ILs systems extends to several hundred-ps/sub-ns. These slow dynamics were attributed by Maroncelli and co-workers[7] to the resistance of the charge-ordered structure of the ILs to reorganization.

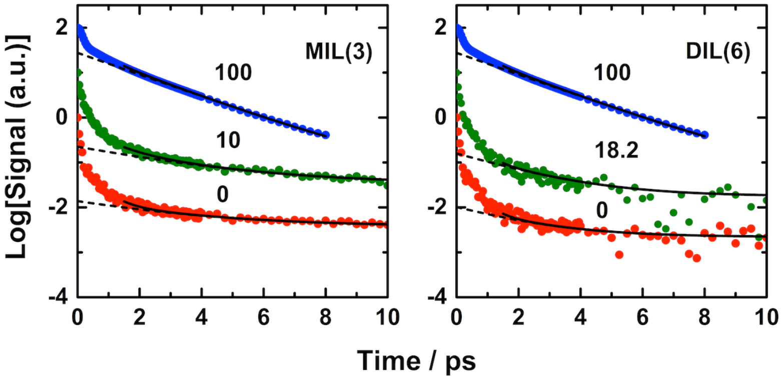

Figure S2. Comparison of representative OHD-RIKES signals in the 0-10 ps time range for (a) the neat CS_2, 10 mol.% CS_2/MIL(3), neat MIL(3); and (b) neat CS_2, 18.2 mol.% CS_2/DIL(6), neat DIL(6). The signals have been normalized at the coherent spike at $t = 0$ and vertically shifted by log-base 10 increments for clarity. The solid black lines are fits of eq 1 to OHD-RIKES decay in 1.5-10 ps time range. Dashed lines are the part of the fit associated with the τ_2-term and the constant B in eq 1. See Table 1 for fit parameters.

III. Analysis of the OHD-RIKES Time-Domain Data

The first step in the procedure for obtaining the reduced response involves fitting OHD-RIKES signals in the 1.5 to 10 ps time range by the empirical decay function

$$r(t) = A_1 exp\left(-\frac{t}{\tau_1}\right) + A_2 \exp\left(-\frac{t}{\tau_2}\right) + B \tag{S1}$$

where the τ_1-terms are sub-picosecond components, the τ_2-term is a picosecond component, and B is a constant that accounts for components in the reorientational dynamics relaxing on a time scale much longer than the time-range of the measurements. The solid lines in Figure 2 are fits of eq 1 with fit parameters for CS_2/IL mixtures tabulated in Table S1. The dashed lines represent the slow contribution to the decays associated with τ_3-term and the constant B. Fit parameters for the OHD-RIKES signals of the other mixtures are given in Table S1.

Table S1. OHD-RIKES decay parameters for CS_2/IL liquid mixtures.[a-c]

CS_2 mol.%	A_1	τ_1 / ps	A_2	τ_2 / ps	B	χ^2
Neat CS_2						
100	0.29	0.62	0.282	1.79	0	0.9999
CS_2/MIL(3)						
0	0.072	0.5	0.01	3.1	0.004	0.9575
10	0.048	0.77	0.019	3.1	0.003	0.9576
15	0.20	0.41	0.034	2.5	0.006	0.9940
20	0.13	0.62	0.024	3.3	0.003	0.9940
25	0.18	0.49	0.042	2.4	0.005	0.9962
CS_2/DIL(6)						
0	0.079	0.36	0.008	2.0	0.002	0.9555
18.2	0.137	0.34	0.019	2.0	0.002	0.9829
26	0.14	0.41	0.017	1.9	0.002	0.9800
33.3	0.14	0.41	0.018	2.4	0.002	0.9896
40	0.13	0.52	0.024	2.4	0.006	0.9907
CS_2/MIL(4)						
0	0.071	0.43	0.013	2.1	0.004	0.9521
10	0.100	0.53	0.017	3.0	0.003	0.9449
15	0.10	0.61	0.022	3.1	0.003	0.9933
20	0.12	0.65	0.027	3.1	0.003	0.995
25	0.20	0.49	0.044	2.5	0.005	0.9965
CS_2/DIL(8)						
0	0.098	0.29	0.005	3.4	0.001	0.9400
18.2	0.16	0.33	0.027	1.5	0.003	0.9901
26	0.16	0.33	0.027	1.5	0.003	0.9901
33.3	0.30	0.42	0.043	2.3	0.005	0.9926
40	0.17	0.43	0.021	2.4	0.003	0.9953
CS_2/MIL(5)						
0	0.011	0.38	0.009	3.0	0.002	0.9457
10	0.10	0.07	0.025	2.3	0.003	0.9348
15	0.09	0.56	0.021	2.7	0.005	0.9935
20	0.14	0.45	0.038	2.2	0.004	0.9840
25	0.14	0.56	0.030	2.7	0.004	0.9972
CS_2/DIL(10)						
0	0.117	0.29	0.008	2.3	0.001	0.9508
18.2	0.198	0.32	0.025	1.6	0.003	0.9897
26	0.20	0.32	0.025	1.6	0.003	0.9897
33.3	0.087	0.55	0.020	2.1	0.003	0.9929
40	0.17	0.48	0.026	2.2	0.003	0.9945

[a] See eq S1 for definitions of fit parameters; fit range 1.5-10 ps. [b] Errors in fit parameters are less than 6%. [c] The imidazolium ring concentration is same in 10 mol.% monocationic ILs (MIL(*n*)) solutions and 18.2 mol.% in dicationic ILs (DIL(2*n*)) solutions.

IV. RSDs and Fits of the Additivity Model to the RSDs

By convoluting the part of the decay given by τ_2-term and the constant B with the pulse intensity autocorrelation, a reorientational response is generated which is then subtracted from the OHD-RIKES signal to yield the reduced response comprising only the electronic and the sub-picosecond nuclear responses. By applying the Fourier-transform-deconvolution procedure to the reduced response, the RSD corresponding to the part of the OKE spectrum associated with intramolecular and subpicosecond intermolecular modes of the liquid is obtained.[8,9] Application of a window function[10] reduces the noise in the low-frequency band in the 0-200 cm^{-1} region of the RSD without affecting its line-shape. Figures S3a-c show the RSDs and fits of the RSDs to the additivity model (eqs 3-7) for 10-25 mol.% CS_2/[C_3C_1im][NTf_2], CS_2/[C_4C_1im][NTf_2], and CS_2/[C_5C_1im][NTf_2] mixtures. Figures S4a-c show the RSDs and fits of the RSDs to the additivity model for 18.2-40 mol.% CS_2/[$(C_1im)_2C_6$][NTf_2]$_2$, CS_2/[$(C_1im)_2C_8$][NTf_2]$_2$, and CS_2/[$(C_1im)_2C_{10}$][NTf_2]$_2$ mixtures. Fit parameters for the Bucaro-Litovitz (BL) and antisymmetrized Gaussian (AG) line-shape functions (eqs 6 and 7) are given Tables S2a-c.

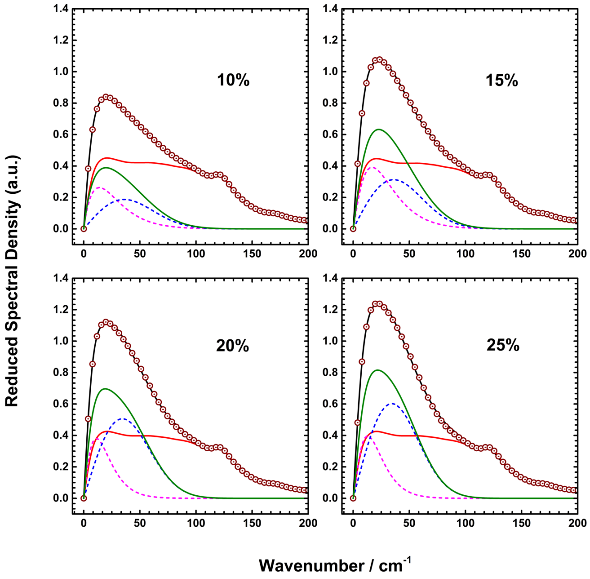

Figure S3a. Reduced spectral densities of 10-25 mol.% CS_2/[C_3C_1im][NTf_2] mixtures with fits of the additivity model (eq 5). Green curves are the CS_2 contributions. Red curves are the IL contributions. The component bands used in the fits of CS_2 contribution are shown. The dashed red curves represent the Bucaro-Litovitz line shape functions and the dashed blue curves the antisymmetrized Gaussian line shape function.

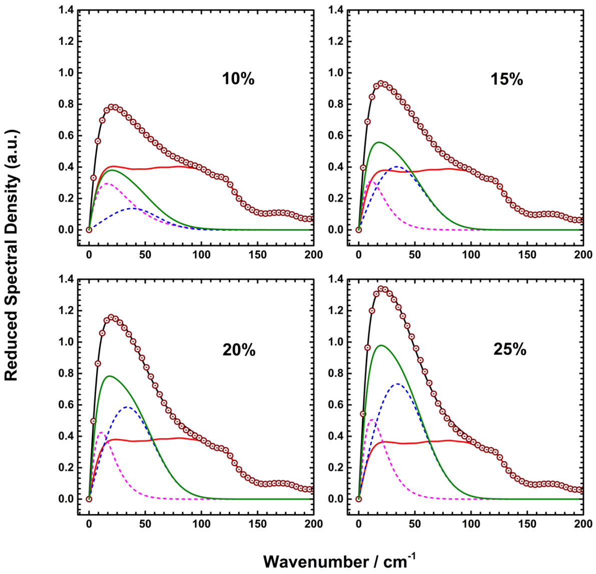

Figure S3b. Reduced spectral densities of 10-25 mol.% CS_2/[C_4C_1im][NTf_2] mixtures with fits of the additivity model (eq 5). Green curves are the CS_2 contributions. Red curves are the IL contributions. The component bands used in the fits of CS_2 contribution are shown. The dashed red curves represent the Bucaro-Litovitz line shape functions and the dashed blue curves the antisymmetrized Gaussian line shape function.

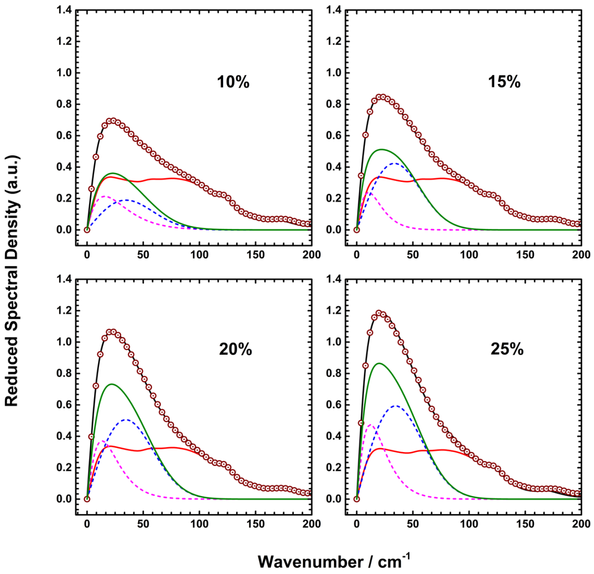

Figure S3c. Reduced spectral densities of 10-25 mol.% CS_2/[C_5C_1im][NTf_2] mixtures with fits of the additivity model (eq 5). Green curves are the CS_2 contributions. Red curves are the IL contributions. The component bands used in the fits of CS_2 contribution are shown. The dashed red curves represent the Bucaro-Litovitz line shape functions and the dashed blue curves the antisymmetrized Gaussian line shape function.

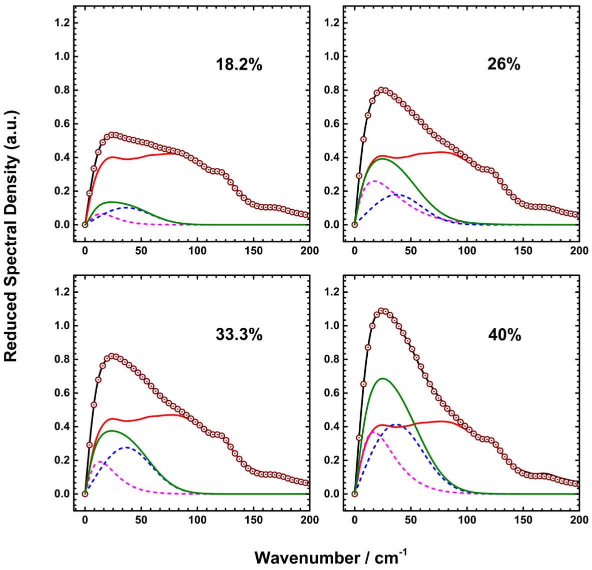

Figure S4a. Reduced spectral densities of 18.2-40 mol.% CS_2/[$(C_1im)_2C_6$][NTf_2]$_2$ mixtures with fits of the additivity model (eq 5). Green curves are the CS_2 contributions. Red curves are the IL contributions. The component bands used in the fits of CS_2 contribution are shown. The dashed red curves represent the Bucaro-Litovitz line shape functions and the dashed blue curves the antisymmetrized Gaussian line shape function.

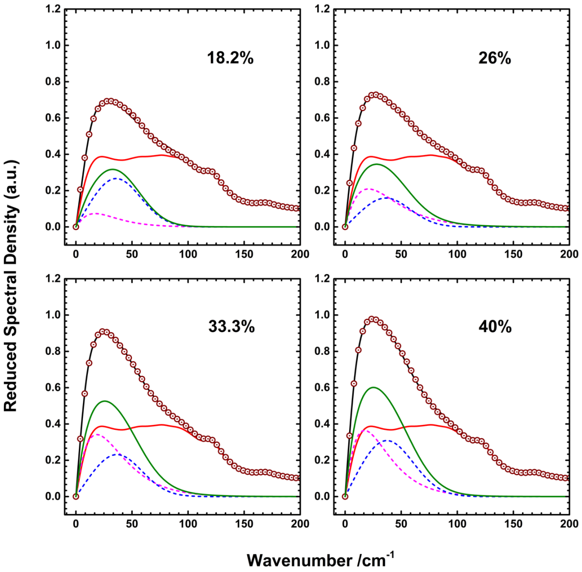

Figure S4b. Reduced spectral densities of 18.2-40 mol.% CS_2/[$(C_1im)_2C_8$][NTf_2]$_2$ mixtures with fits of the additivity model (eq 5). Green curves are the CS_2 contributions. Red curves are the IL contributions. The component bands used in the fits of CS_2 contribution are shown. The dashed red curves represent the Bucaro-Litovitz line shape functions and the dashed blue curves the antisymmetrized Gaussian line shape function.

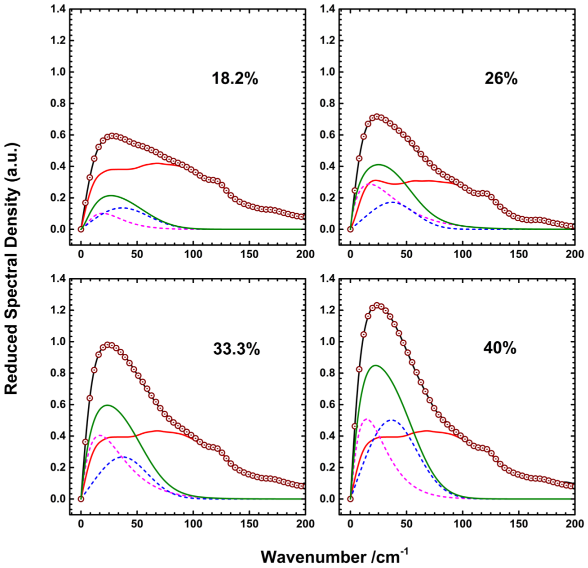

Figure S4c. CS_2/[(C_1im)$_2C_{10}$][NTf_2]$_2$ mixtures with fits of the additivity model (eq 5). Green curves are the CS_2 contributions. Red curves are the IL contributions. The component bands used in the fits of CS_2 contribution are shown. The dashed red curves represent the Bucaro-Litovitz line shape functions and the dashed blue curves the antisymmetrized Gaussian line shape function.

Table S2a. Fit parameters of two-component line-shape function to CS_2 intermolecular spectra in 15 mol.% CS_2/MIL(*n*) and 26 mol.% CS_2/DIL(2*n*) mixtures with n = 3-5.[a-c]

System	A_{BL}	a	ω_{BL} / cm^{-1}	f_{BL}	A_{AG}	ω_{AG} / cm^{-1}	ε /cm^{-1}	f_{AG}
MIL(3)	0.039	1.26	13.3	0.47	0.33	32.86	27.7	0.53
MIL(4)	0.044	1.38	8.002	0.27	0.418	31.78	25.2	0.73
MIL(5)	0.038	1.36	7.7	0.21	0.438	31.62	24.4	0.79
DIL(6)	0.039	1.00	16.8	0.57	0.180	37.00	22.4	0.43
DIL(8)	0.023	1.10	19.0	0.59	0.160	35.95	22.0	0.41
DIL(10)	0.061	0.84	20.0	0.64	0.172	36.88	20.4	0.36

[a] From fit of the additivity model (eqs 3 and 5) to RSDs. See eqs 6 and 7 for definitions of A_{BL}, a, ω_{BL}, A_{AG}, ω_{AG} and ε.

[b] Fractional areas of component bands - f_{BL}, f_{AG}.

[c] Errors in fit parameters: A_{BL}± 0.0007; a ±0.005; ω_{BL} ± 0.6; A_{AG} ± 0.004; ω_{AG} ±0 .34; ε ± 0.3.

Table S2b. Fit parameters of two-component line-shape function to CS_2 intermolecular spectra in 20 mol.% CS_2/MIL(*n*) and 33.3 mol.% CS_2/DIL(2*n*) mixtures with n = 3-5.[a-c]

System	A_{BL}	a	ω_{BL} / cm^{-1}	f_{BL}	A_{AG}	ω_{AG} / cm^{-1}	ε /cm^{-1}	f_{AG}
MIL(3)	0.061	1.30	8.6	0.27	0.530	31.73	26.0	0.73
MIL(4)	0.059	1.42	7.7	0.26	0.607	31.79	24.8	0.74
MIL(5)	0.044	1.35	9.8	0.30	0.529	31.86	26.0	0.70
DIL(6)	0.023	1.30	9.6	0.29	0.278	35.85	23.0	0.71
DIL(8)	0.045	1.00	17.7	0.59	0.233	36.12	22.6	0.41
DIL(10)	0.061	1.04	16.1	0.57	0.268	36.77	22.3	0.43

[a] From fit of the additivity model (eqs 3 and 5) to RSDs. See eqs 6 and 7 for definitions of A_{BL}, a, ω_{BL}, A_{AG}, ω_{AG} and ε.

[b] Fractional areas of component bands - f_{BL}, f_{AG}.

[c] Errors in fit parameters: A_{BL}± 0.0007; a ±0.005; ω_{BL} ± 0.6; A_{AG} ± 0.004; ω_{AG} ±0 .34; ε ± 0.3.

Table S2c. Fit parameters of two-component line-shape function to CS_2 intermolecular spectra in 25 mol.% CS_2/MIL(*n*) and 40 mol.% CS_2/DIL(2*n*) mixtures with *n* = 3-5.[a-c]

System	A_{BL}	a	ω_{BL} / cm^{-1}	f_{BL}	A_{AG}	ω_{AG} / cm^{-1}	ε /cm^{-1}	f_{AG}
MIL(3)	0.037	1.52	8.5	0.26	0.62	32.69	24.8	0.74
MIL(4)	0.062	1.45	8.03	0.25	0.759	32.24	25.2	0.75
MIL(5)	0.067	1.3	9.3	0.30	0.619	32.05	25.9	0.70
DIL(6)	0.027	1.43	11.8	0.38	0.42	35.82	24.6	0.62
DIL(8)	0.046	1.1	15.6	0.50	0.312	36.49	24.0	0.50
DIL(10)	0.071	1.18	12.2	0.41	0.506	35.98	23.1	0.59

[a] From fit of the additivity model (eqs 3 and 5) to RSDs. See eqs 6 and 7 for definitions of A_{BL}, a, ω_{BL}, A_{AG}, ω_{AG} and ε.

[b] Fractional areas of component bands - f_{BL}, f_{AG}.

[c] Errors in fit parameters: $A_{BL} \pm 0.0007$; a ±0.005; $\omega_{BL} \pm 0.6$; $A_{AG} \pm 0.004$; ω_{AG} ±0 .34; $\varepsilon \pm 0.3$.

Table S3. Two-Component Model -- Antisymmetrized Gaussian Frequency, ω_{AG}.

MIL/DIL %	MIL(3) cm^{-1}	DIL(6) cm^{-1}	MIL(4) cm^{-1}	DIL(8) cm^{-1}	MIL(5) cm^{-1}	DIL(10) cm^{-1}
10/18.2	32.86	36.03	32.33	35.41	31.96	35.82
15/26	32.86	37.00	31.78	35.95	31.62	36.88
20/33.3	31.73	35.85	31.79	36.12	31.86	36.77
25/40	32.69	35.82	32.24	36.49	32.05	35.98
Statistics						
average	32.54	36.18	32.04	35.99	31.87	36.37
std	0.54	0.56	0.29	0.45	0.19	0.54
avg(std)	32.5(5)	36.2(6)	32.0(3)	36.0(5)	31.9(2)	36.4(5)

References

1 S. V. Dzyuba and R. A. Bartsch, Efficient Synthesis of 1-Alkyl(aralkyl)-3-methy(ethyl)imidazolium Halides: Precursors for Room Temperature Ionic Liquids, *J. Heterocyclic Chem.*, 2001, **38**, 265-268.

2 S. V. Dzyuba and R. A. Bartsch, Influence of Structural Variations in 1-Alkyl(aralky)-3-methylimidazolium Hexaphosphates and Bis[(trifluoromethane)sulfonyl]amides on Physical Properties of the Ionic Liquids, *ChemPhysChem*, 2002, **3**, 161-166.

3 P. Bonhote, A.-P. Dias, N. Papageorgiou, K. Kalyansundaram and M. Gratzel, Hydrophobic, Highly Conductive Ambient-Temperature Molten Salts, *Inorg. Chem.*, 1996, **35**, 1168-1178.

4 H. Cang, L. Jie and M. D. Fayer, Orientational Dynamics of the Ionic Liquid 1-Ethyl-3-Methylimidazolium Nitrate, *J. Chem. Phys.*, 2003, **119**, 13017-13023.

5 B. G. Nicolau, A. Sturlaugson, K. Fruchey, M. C. C. Ribeiro and M. D. Fayer, Room Temperature Ionic Liquid-Lithium Salt Mixtures: Optical Kerr Effect Dynamical Measurements, *J. Phys. Chem. B*, 2010, **114**, 8350-8356.

6 D. A. Turton, J. Hunger, A. Stoppa, G. Hefter, A. Thoman, M. Walther, R. Buchner and K. Wynne, Dynamics of Imidazolium Ionic Liquids from a Combined Dielectric Relaxation and Optical Kerr Effect Study: Evidence for Mesoscopic Aggregation, *J. Am. Chem. Soc.*, 2009, **131**, 11140-11146.

7 D. Roy, N. Patel, S. Conte and M. Maroncelli, Dynamics in an Idealized Ionic Liquid Model, *J. Phys. Chem. B*, 2010, **114**, 8410-8424.

8 D. McMorrow, Separation of Nuclear and Electronic Contributions to Femtosecond Four-Wave Mixing Data, *Opt. Commun.*, 1991, **86**, 236-244.

9 D. McMorrow and W. T. Lotshaw, Intermolecular Dynamics in Acetonitrile Probed with Femtosecond Fourier Transform Raman Spectroscopy, *J. Phys. Chem.*, 1991, **95**, 10395-10406.

10 P. Yang, G. A. Voth, D. Xiao, L. G. Hines Jr., R. A. Bartsch and E. L. Quitevis, Nanostructural Organization in Carbon Disulfide/Ionic Liquid Mixtures: Molecular Dynamics Simulations and Optical Kerr Effect Spectroscopy, *J. Chem. Phys.*, 2011, **135**, 034502(1)-034502(12).